Nuclear Science and Techniques (2025) 36:205
https://doi.org/10.1007/s41365-025-01778-1

Dineutron and diproton correlations in the exotic nuclei ^{6}He and ^{6}Be

Xiao-Quan Du[1] · Cong-Wu Wang[1,2] · De-Ye Tao[1] · Bo Zhou[1,3] · Yu-Gang Ma[1,3]

Received: 4 February 2025 / Revised: 15 March 2025 / Accepted: 31 March 2025 / Published online: 14 August 2025

Abstract
To investigate the structural configuration of ^{6}He and ^{6}Be in a three-cluster system and to highlight dinucleon correlations, we performed a two-cluster overlap amplitude (TCOA) calculation, which is an extension of the RWA formalism. The total wave functions were obtained using the generator coordinate method with microscopic cluster wave functions. Based on these wave functions, we calculated the overlap amplitudes to extract the relative motion and spatial correlations between clusters. The computed energy spectra showed reasonable agreement with the experimental data, emphasizing the effectiveness of the present framework for investigating dinucleon correlations in light nuclei. Our results revealed the presence of both dinucleon-like and cigar-like configurations in the ground states of ^{6}He and ^{6}Be, indicating a coexistence of compact and extended cluster structures. Furthermore, the 2^{+}_{1} state of ^{6}He revealed a pronounced dineutron structure, with strong spatial correlations between the two valence neutrons. We also performed calculations for the higher-lying 2^{+}_{2} state, which showed a more spatially extended structure and provided potential references for future experimental investigations. These findings demonstrated that the TCOA method served as a powerful tool to explore cluster dynamics and dinucleon features in light, weakly bound nuclear systems.

Keywords Diproton · Dineutron · Nuclear cluster model · Halo nuclei · Overlap amplitude

1 Introduction

Clustering is a fundamental phenomenon in the nucleus [1–8]. Cluster models are widely used and have been shown to be effective in describing the characteristics of light nuclei [9, 10]. With the cluster model, the study of diproton and dineutron correlations is crucial for understanding nucleon-nucleon interactions and the underlying nuclear structure, providing information on pairing mechanisms and the behavior of nucleons in short-range interactions, which are essential for understanding phenomena such as nuclear stability and reaction dynamics [11–14].

^{6}He, the lightest Borromean halo nucleus, together with its mirror nucleus ^{6}Be, the lightest two-proton emitter, has attracted extensive studies on the dinucleon correlations in their decaying modes and structures [15–21]. Previous studies have described the structure of ^{6}He [22–24], a more precise description can be found in [25], which addresses both six-body correlations and clustering in the ^{6}He ground state using the no-core shell model with continuum (NCSMC), where the “dineutron" configuration is shown to prevail over the “cigar" structure. Recently, the 2^{+}_{1} state of ^{6}He was suggested to exhibit a dineutron correlation based on simulations of its decay mode [16]. Regarding its mirrored nucleus, ^{6}Be stands out as the lightest two-proton emitter featuring a distinct structure of α and two protons [26, 27]. This characteristic, in accordance with Golandsky’s framework, establishes a robust benchmark for conducting comprehensive

This work was supported by the National Key R&D Program of China (Nos. 2023YFA1606701 and 2022YFA1602402), the National Natural Science Foundation of China (Nos. 12175042, 11890710, 11890714, 12047514, 12147101, and 12347106), Guangdong Major Project of Basic and Applied Basic Research (No. 2020B0301030008), and the 111 Project.

✉ Bo Zhou
zhou_bo@fudan.edu.cn

Yu-Gang Ma
mayugang@fudan.edu.cn

[1] Key Laboratory of Nuclear Physics and Ion-beam Application (MOE), Institute of Modern Physics, Fudan University, Shanghai 200433, China

[2] Institut für Theoretische Physik II, Ruhr-Universität Bochum, 44780 Bochum, Germany

[3] Shanghai Research Center for Theoretical Nuclear Physics, NSFC and Fudan University, Shanghai 200438, China

investigations of two-proton decay and diproton correlations within nuclear structure [28, 29].

Dineutron and diproton correlations have been intensively discussed through 2n and 2p emissions from unbound nuclei in connection with recent experiments [30–33]. In the case of ^{6}He, experiments have investigated the decay mode of its 2_1^+ resonant state via the ^{6}He breakup reaction by ^{12}C at 240 MeV/nucleon, revealing the coexistence of dineutron decay and democratic decay, which suggests the possible existence of a dineutron structure in the 2_1^+ state of ^{6}He [34]. For ^{6}Be, experiments using a high-resolution array to detect its α+p+p three-body decay have provided precise three-body correlation data that agree well with theoretical models, thereby validating the theoretical approach over a wide range of energies [13, 28, 35–38].

The main objective of this study was to investigate the correlations between diprotons and dineutrons in ^{6}He and ^{6}Be in several low-lying states of ^{6}He and ^{6}Be at the structural level using a microscopic nuclear model. We employed the generator coordinate method (GCM) with Brink wave functions [39, 40] as a robust framework to model and analyze these correlations.

By calculating the two-cluster overlap amplitude (TCOA), we aim to quantify the spatial distribution and correlation strength of nucleon pairs, providing insights into the nucleon-nucleon interactions within these nuclei [41, 42]. This approach enables detailed examination of the structural and correlation properties of ^{6}He and ^{6}Be, contributing to a deeper understanding of nucleon correlations in light nuclear systems [43, 44].

2 Theoretical framework

In the present GCM calculations, the total wave function of ^{6}He (^{6}Be) can be written as the superposition of angular-momentum-projected and parity-projected Brink wave functions

$$\Psi_M^{J\pi} = \sum_{i,K} c_{i,K} \hat{P}^J_{MK} \hat{P}^{\pi} \Phi^{\mathrm{B}}(\{\boldsymbol{R}\}_i), \tag{1}$$

where $\hat{P}^J_{MK}$ and $\hat{P}^{\pi}$ are the angular-momentum and parity projectors, respectively. The index i indicates a specified set of generator coordinates $\{R_1, R_2, R_3\}$. An illustration of ^{6}He is shown in Fig. 1. The Brink wave function is fully antisymmetrized, and the wave function of the k-th nucleon is defined as a Gaussian wave packet

$$\phi_k(\boldsymbol{R}_j) = \frac{1}{(\pi b^2)^{3/4}} \exp\left[-\frac{1}{2b^2}(\boldsymbol{r}_k - \boldsymbol{R}_j)^2\right] \chi_k \tau_k. \tag{2}$$

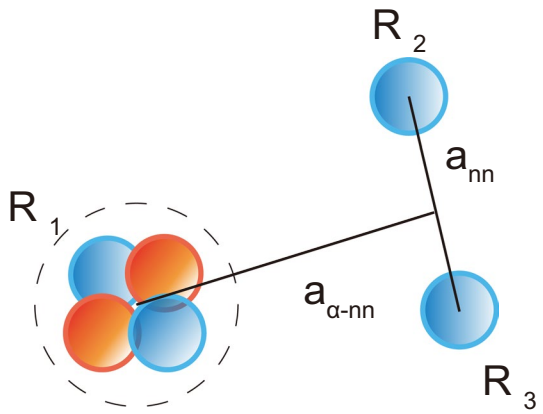

Fig. 1 (Color online) Schematic diagram of α+n+n clustering structure of the Brink wave function of ^{6}He

In the present calculation, the oscillator parameter for the single-particle wave functions was set to $b = 1.46$ fm, which is the same as that used in Refs. [45, 46]. The Hamiltonian of the system includes kinetic, central N-N, spin-orbit, and Coulomb parts

$$\hat{H} = -\frac{\hbar^2}{2m}\sum_i \nabla_i^2 - T_{\mathrm{c.m.}} + \sum_{i<j} \hat{V}_{ij}^{\mathrm{NN}} + \sum_{i<j} \hat{V}_{ij}^{\mathrm{LS}} + \sum_{i<j} \hat{V}_{ij}^{\mathrm{C}}. \tag{3}$$

The Volkov No.2 potential [47] was taken as the central N-N potential

$$\hat{V}_{ij}^{\mathrm{NN}} = \sum_{n=1}^{2} v_n e^{-\frac{r_{ij}^2}{a_n^2}} (W + B\hat{P}_{\sigma} - H\hat{P}_{\tau} - M\hat{P}_{\sigma}\hat{P}_{\tau})_{ij} \tag{4}$$

with $a_1 = 1.01$ fm, $a_2 = 1.8$ fm, $v_1 = 61.14$ MeV, $v_2 = -60.65$ MeV, $W = 1 - M, M = 0.6$ and $B = H = 0.125$. The G3RS potential [48, 49] is used for the spin-orbit term

$$\hat{V}_{ij}^{\mathrm{LS}} = v_0(e^{-d_1 r_{ij}^2} - e^{-d_2 r_{ij}^2})\hat{P}(^3O)\boldsymbol{L}\cdot\boldsymbol{S}, \tag{5}$$

where $\hat{P}(^3O)$ is the projection operator onto a triplet odd state, strength $v_0 = 2000$ MeV, and parameters d_1 and d_2 are set to 5.0 fm^{-2} and 2.778 fm^{-2}, respectively. The coefficients $\{c_{i,K}\}$ in Eq. (1) are determined by solving the Hill–Wheeler equation as follows:

TCOA was introduced as an extension of the RWA method to quantitatively analyze the spatial distribution and correlation strength of nucleon pairs [50]. This approach has been successfully applied to study core + $N + N + N$ structures [51], providing a detailed description of clustering dynamics.

To illustrate the three-cluster structure, the TCOA [52] of ^{6}He is defined as:

$$\mathcal{Y}^{J^\pi}_{l_1 l_{23} L}(a_{\alpha-nn}, a_{nn}) = \sqrt{\frac{6!}{4!1!1!}} \left\langle \frac{\delta(r_1 - a_{\alpha-nn})\delta(r_{23} - a_{nn})}{r_1^2 r_{23}^2} \left[[Y_{l_1}(\hat{r}_1) \otimes Y_{l_{23}}(\hat{r}_{23})]_L \otimes [\Phi_\alpha \otimes \Phi_n \otimes \Phi_n]_0 \right]_{JM} | \Psi^{J^\pi}_M \right\rangle \quad (6)$$

where $a_{\alpha-nn}$ and a_{nn} represent the distances from the center of mass(c.o.m.) of the two neutrons to the α cluster, and the distance between the two neutrons, respectively, as shown in Fig. 1. l_1 and l_{23} correspond to the orbital angular momenta associated with distances $a_{\alpha-nn}$ and a_{nn}, respectively, while L denotes the total angular momentum obtained from their coupling. The reference wave function for the α cluster is denoted by Φ_α.

To characterize the relative motion between the α cluster and the two neutrons, we introduce the relative-motion coordinates r_1 and r_{23}, which are defined as

$$r_1 = \mathbf{X}_1 - \frac{\mathbf{X}_2 + \mathbf{X}_3}{2}, \quad r_{23} = \mathbf{X}_2 - \mathbf{X}_3, \quad (7)$$

where $\mathbf{X}_i$ is the c.o.m. of the physical coordinates of the α and neutrons. (Similarly, the structure of ^{6}Be is analogous, with two valence neutrons replaced by two valence protons.)

The TCOA provides the spatial distribution of valence nucleons in terms of the distance between the two valence nucleons, a_{NN}, and the distance between their center and the α-core nucleus, $a_{\alpha-NN}$. It should be noted that the other degrees of freedom are integrated into in Eq. 6. The description provided by the TCOA can be viewed as the averaged isosceles triangle configuration. This allows us to estimate the opening angle $\theta = 2\arctan(a_{NN}/2a_{\alpha-NN})$, of the two nucleons with respect to the core. The opening angle θ is a key measure for dinucleon correlations; for instance, $\theta = 90°$ corresponds to two non-correlated nucleons.

3 Results and discussion

By superposing 600 distinct three-body spatial configurations, α + n + n and α + p + p, we obtained clustering wave functions for both ^{6}He and ^{6}Be. The resulting positive-parity low-lying state energy spectra are shown in Fig. 2, exhibiting an overall shift compared with the experimental data. The calculated positive-parity low-lying energy spectra (Fig. 2) exhibited qualitative consistency with the experimentally observed 0^+ and 2^+ states. For example, the calculated excitation energy of the 2^+_1 state for ^{6}He agrees well with the experimental observations—corresponding to very narrow resonances—showing only a small deviation of approximately 0.3 MeV. Moreover, the mirror symmetry breaking for ^{6}He and ^{6}Be in the ground state energy

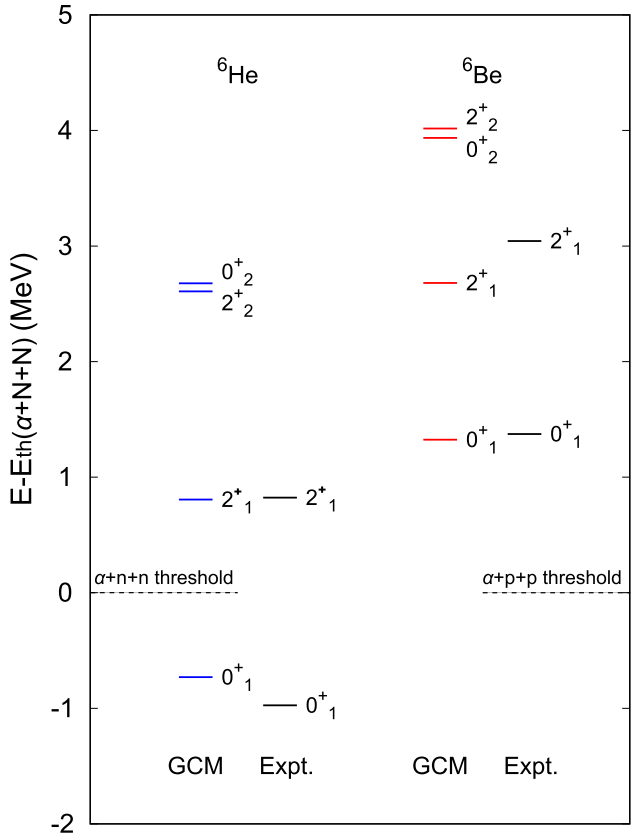

Fig. 2 The calculated energy spectra of ^{6}He and ^{6}Be compared with the corresponding experimental values. The gray dashed lines represent thresholds

was also well reproduced. This consistency indicates that mirror symmetry breaking caused by isospin effects and Coulomb interactions, as well as the spatial extension of the valence nucleons, is effectively described. In the following section, we focus on the detailed spatial distribution of the valence nucleons relative to the α-core nucleus.

Based on the definition of the TCOA discussed above, this framework effectively characterizes critical three-body cluster correlations, with specific emphasis on the dineutron correlation in ^{6}He and the diproton correlation in ^{6}Be. Figures 3 and 4 present the TCOA distributions for three-cluster systems in ^{6}He and ^{6}Be, where the orbital angular momenta quantum numbers $l_1 = l_{23} = 0$ and $l_1 = l_{23} = 1$ were chosen because these specific combinations exhibited the most pronounced TCOA distribution amplitudes. In a purely non-correlated scenario, the distributions would exhibit equal weights on both sides of the dashed lines in the figure, which divide two distinct regions in the hyperspherical description of three-body nuclei [53]. For the ground states of ^{6}He and ^{6}Be, two distinct peaks were observed: a dinucleon-like peak in the region $a_{\alpha-NN} > a_{NN}/2$ and a cigar-like peak in the region $a_{\alpha-NN} < a_{NN}/2$. These peaks arise from the two valence

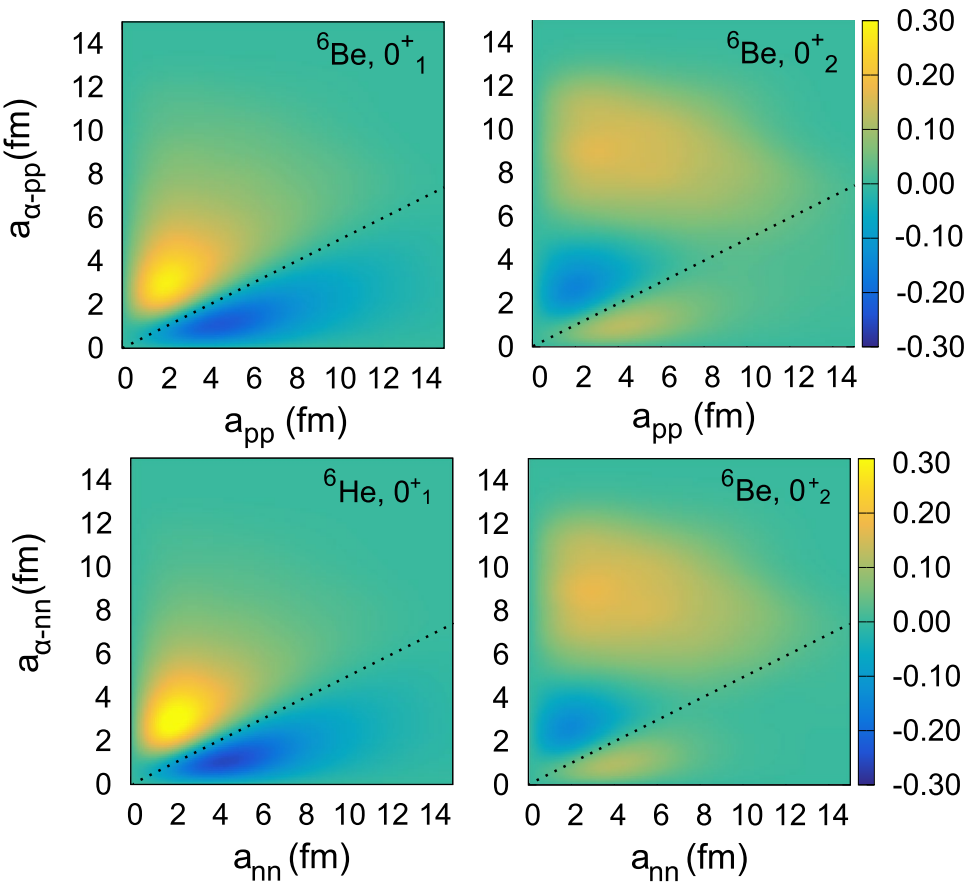

Fig. 3 (Color online) TCOA calculation for the ground states of ^{6}Be and ^{6}He. The internal orbital angular momenta are $l_1 = 0$ and $l_{23} = 0$. The dashed line represents $a_{\alpha-\mathrm{NN}} = a_{\mathrm{NN}}/2$

nucleons that predominantly occupy the *p*-shell. The TCOA further indicates that a dinucleon-like configuration is favored, as evidenced by its higher maximum TCOA and asymmetric distribution. For example, in ^{6}He, the dineutron-like peak is characterized by $\mathcal{Y}^{J^\pi}_{l_1 l_{23} L}(\{a_{\alpha-\mathrm{nn}}, a_{\mathrm{nn}}\} = \{2.1\,\mathrm{fm}, 3\,\mathrm{fm}\}) = 0.32$, which is consistent with the *ab initio* results in Ref. [25], whereas the cigar-like peak is given by $\mathcal{Y}^{J^\pi}_{l_1 l_{23} L}(\{a_{\alpha-\mathrm{nn}}, a_{\mathrm{nn}}\} = \{4.4\,\mathrm{fm}, 1.1\,\mathrm{fm}\}) = -0.26$.

The conclusion of the favored dineutron correlation in the ground state of ^{6}He is consistent with a recent experimental work [15], which extracted B(E1) values to infer an average opening angle of the two valence neutrons of approximately 56°, supporting the presence of a dineutron correlation. The TCOA for ^{6}Be exhibits similar behavior, with a maximum characterized by $\mathcal{Y}^{J^\pi}_{l_1 l_{23} L}(\{a_{\alpha-\mathrm{pp}}, a_{\mathrm{pp}}\} = \{2.1\,\mathrm{fm}, 3\,\mathrm{fm}\}) = 0.28$, and another peak given by $\mathcal{Y}^{J^\pi}_{l_1 l_{23} L}(\{a_{\alpha-\mathrm{pp}}, a_{\mathrm{pp}}\} = \{4.5\,\mathrm{fm}, 1.1\,\mathrm{fm}\}) = -0.23$. However, the peak amplitudes are suppressed owing to the Coulomb repulsion. Additionally, a halo(-like) nature was revealed in the TCOA, as indicated by the diffuse distribution. For ^{6}He and ^{6}Be, the TCOA extends up to $a_{\alpha-\mathrm{NN}} \approx 10\,\mathrm{fm}$, whereas heavier ^{10}Be exhibits a more compact distribution using a 2n overlap function [54].

Compared to the ground states, the 0^+_2 states of both ^{6}He and ^{6}Be, there are mainly three main peak regions: dineucleon-like and cigar-like retained, while a stronger third peak emerged in the acute opening angle region. The three peaks might be due to significant *d*−wave occupation in the 0^+_2 states; for example, the ground state in ^{18}O nucleus in [55]. Compared with the ground state, this state is more diffuse and exhibits a gas-like feature, which indicates a more complex correlation structure.

For the first excited state 2^+_1 in both ^{6}He and ^{6}Be, as shown in Fig. 4, we found that there was only one peak, predominantly distributed in the dineucleon correlation region, that is, $a_{\mathrm{NN}} > 2a_{\alpha-\mathrm{NN}}$ ($\theta_{\mathrm{NN}} = 2\arctan(a_{\mathrm{NN}}/2a_{\alpha-\mathrm{NN}}) < 90°$). The maximum value is characterized by $\mathcal{Y}^{J^\pi}_{l_1 l_{23} L}(\{a_{\alpha-\mathrm{nn}}, a_{\mathrm{nn}}\} = \{3.8\,\mathrm{fm}, 2.1\,\mathrm{fm}\}) = 0.16$ for ^{6}He, corresponding to an opening angle of $\theta_{\mathrm{NN}} = 85°$. This result is consistent with a recent three-body model calculation using the complex-scaling method, which shows a peak in the opening angle density profile at approximately $60° \sim 80°$. For ^{6}Be, the peak is characterized by $\mathcal{Y}^{J^\pi}_{l_1 l_{23} L}(\{a_{\alpha-\mathrm{pp}}, a_{\mathrm{pp}}\} = \{4.0\,\mathrm{fm}, 2.2\,\mathrm{fm}\}) = 0.13$, with a noticeably smaller amplitude. This difference represents the observed mirror symmetry breaking in the dineucleon correlations, where the effects of the Coulomb interaction result in a weaker diproton correlation.

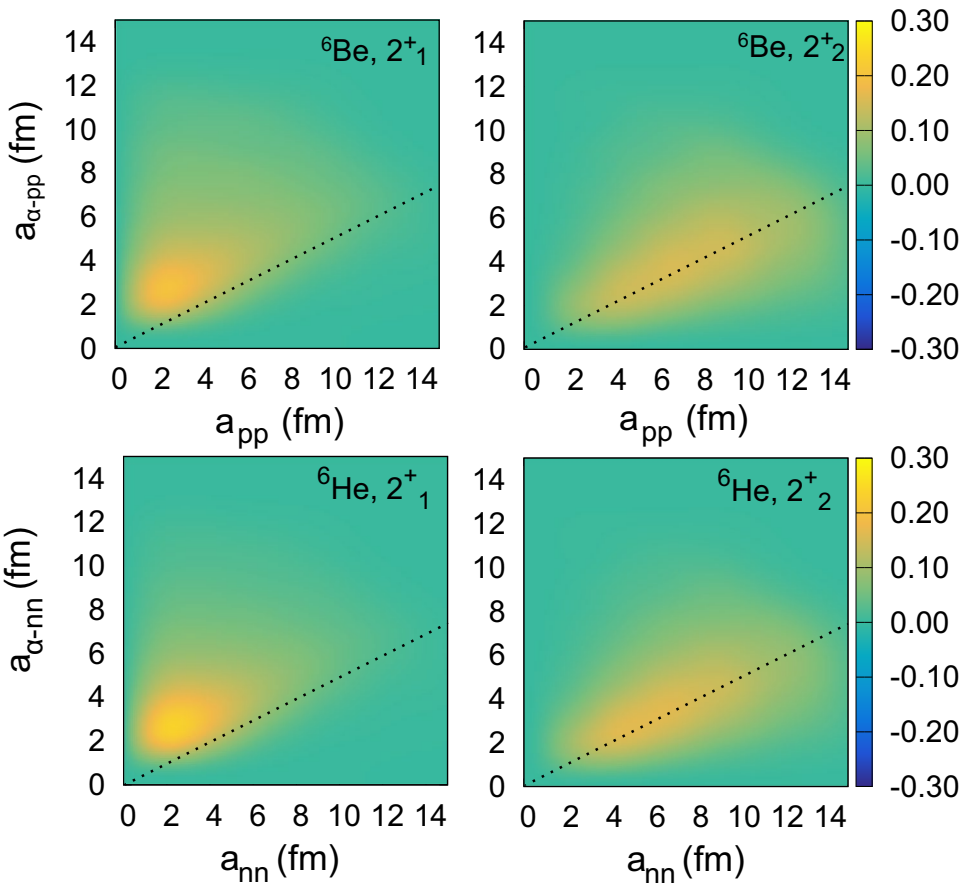

Fig. 4 (Color online) TCOA calculation for the 2^+ states of ^{6}Be and ^{6}He. The internal orbital angular momenta are $l_1 = 1$ and $l_{23} = 1$. The dashed line represents $a_{\alpha-\mathrm{NN}} = a_{\mathrm{NN}}/2$

The TCOA distributions of the 2^+_2 states in both ^{6}Be and ^{6}He exhibited remarkably similar gas-like characteristics, manifested as diffuse patterns without distinct peaks. Notably, both nuclei showed a single dominant peak in their respective distributions, with suppressed two-nucleon correlations compared to their 2^+_1 states. For ^{6}Be, this corresponds to a weakened diproton correlation in the 2^+_2 state, whereas for ^{6}He the analogous suppression occurs in the dineutron component.

4 Summary

In this study, we investigated the diproton and dineutron correlations in the ground and low-lying 2^+ states of ^{6}Be and ^{6}He using the TCOA method within the GCM framework. Our calculations reveal that both ^{6}Be and ^{6}He exhibit pronounced diproton and dineutron correlations in their ground states, characterized by a cigar-like spatial configuration with a localized nucleon pair. The TCOA distributions for the 2^+_1 states also show a single-peak structure, which is indicative of dinucleon correlations consistent with previous descriptions.

The present theoretical framework, combining the GCM with TCOA analysis, has proven effective in providing a detailed description of nucleon-nucleon correlations and clustering behavior in light nuclear systems, offering insights into the structural evolution of mirror nuclei across different excitation energies.

Author Contributions All authors contributed to the study conception and design. Material preparation, data collection and analysis were performed by Xiao-Quan Du and Bo Zhou. The first draft of the manuscript was written by Xiao-Quan Du, and all authors commented on previous versions of the manuscript. All authors read and approved the final manuscript.

Declarations

Conflict of interest Yu-Gang Ma is the editor-in-chief for Nuclear Science and Techniques and was not involved in the editorial review, or the decision to publish this article. All authors declare that there are no conflict of interest.

References

1. M. Freer, H. Horiuchi, Y. Kanada-En'yo et al., Microscopic clustering in light nuclei. Rev. Mod. Phys. **90**, 035004 (2018). https://doi.org/10.1103/RevModPhys.90.035004

2. B. Zhou, Y. Funaki, H. Horiuchi et al., Nonlocalized clustering: a new concept in nuclear cluster structure physics. Phys. Rev. Lett. **110**, 262501 (2013). https://doi.org/10.1103/PhysRevLett.110.262501
3. Y. Ye, X. Yang, H. Sakurai et al., Physics of exotic nuclei. Nat. Rev. Phys. **7**, 21–37 (2025). https://doi.org/10.1038/s42254-024-00782-5
4. W.B. He, Y.G. Ma, X.G. Cao et al., Giant dipole resonance as a fingerprint of α clustering configurations in ^{12}C and ^{16}O. Phys. Rev. Lett. **113**, 032506 (2014). https://doi.org/10.1103/PhysRevLett.113.032506
5. S.S. Wang, Y.G. Ma, D.Q. Fang et al., Effects of neutron-skin thickness on direct hard photon emission from reactions induced by the neutron-rich projectile ^{50}Ca. Phys. Rev. C **105**, 034616 (2022). https://doi.org/10.1103/PhysRevC.105.034616
6. G. Ren, C.W. Ma, X.G. Cao et al., Bubble ^{36}Ar and its new breathing modes. Phys. Lett. B **857**, 138990 (2024). https://doi.org/10.1016/j.physletb.2024.138990
7. Y.G. Ma, Effects of α-clustering structure on nuclear reaction and relativistic heavy-ion collisions. Nucl. Tech. (in Chinese) **46**, 080001 (2023). https://doi.org/10.11889/j.0253-3219.2023.hjs.46.080001
8. Y.G. Ma, S. Zhang, α-clustering effects in relativistic heavy-ion collisions. Sci. Sin. Phys. Mech. Astron. **54**, 292004 (2024). https://doi.org/10.1360/SSPMA-2024-0013. (**in Chinese**)
9. K. Wildermuth, Y.C. Tang, E. Sheldon, A unified theory of the nucleus. Phys. Today **30**, 62–63 (2013). https://doi.org/10.1063/1.3037638
10. W. von Oertzen, M. Freer, Y. Kanada-En'yo, Nuclear clusters and nuclear molecules. Phys. Rep. **432**, 43–113 (2006). https://doi.org/10.1016/j.physrep.2006.07.001
11. G. Bertsch, H. Esbensen, Pair correlations near the neutron drip line. Ann. Phys. **209**, 327–363 (1991). https://doi.org/10.1016/0003-4916(91)90033-5
12. K. Hagino, H. Sagawa, Pairing correlations in nuclei on the neutron-drip line. Phys. Rev. C **72**, 044321 (2005). https://doi.org/10.1103/PhysRevC.72.044321
13. L. Grigorenko, R. Johnson, I. Mukha et al., Two-proton radioactivity and three-body decay: general problems and theoretical approach. Phys. Rev. C **64**, 054002 (2001). https://doi.org/10.1103/PhysRevC.64.054002
14. B. Zhou, Y. Funaki, H. Horiuchi et al., The 5α condensate state in ^{20}Ne. Nat. Commun. **14**, 8206 (2023). https://doi.org/10.1038/s41467-023-43816-9
15. Y. Sun, T. Nakamura, Y. Kondo et al., Three-body breakup of ^{6}He and its halo structure. Phys. Lett. B **814**, 136072 (2021). https://doi.org/10.1016/j.physletb.2021.136072
16. S. Ogawa, T. Matsumoto, Dineutron in the 2^+_1 state of ^{6}He. Phys. Rev. C **105**, L041601 (2022). https://doi.org/10.1103/PhysRevC.105.L041601
17. Y. Kanada-En'yo, H. Feldmeier, T. Suhara, Two-neutron correlations in microscopic wave functions of ^{6}He, ^{8}He, and ^{12}C. Phys. Rev. C **84**, 054301 (2011). https://doi.org/10.1103/PhysRevC.84.054301
18. G. Thiamova, Ground state properties of beryllium isotopes studied by amd+gcm method. Phys. Scr. **71**, 349 (2005). https://doi.org/10.1238/Physica.Regular.071a00349
19. M. Zhukov, B. Danilin, D. Fedorov et al., Bound state properties of Borromean halo nuclei: ^{6}He and ^{11}Li. Phys. Rep. **231**, 151–199 (1993). https://doi.org/10.1016/0370-1573(93)90141-Y
20. L. Zhou, S.M. Wang, D.Q. Fang et al., Recent progress in two-proton radioactivity. Nucl. Sci. Tech. **33**, 105 (2022). https://doi.org/10.1007/s41365-022-01091-1
21. S. Wang, W. Nazarewicz, Fermion pair dynamics in open quantum systems. Phys. Rev. Lett. **126**, 142501 (2021). https://doi.org/10.1103/PhysRevLett.126.142501
22. D. Sääf, C. Forssen, Microscopic description of translationally invariant core+ n+ n overlap functions. Phys. Rev. C **89**, 011303 (2014). https://doi.org/10.1103/PhysRevC.89.011303
23. P. Descouvemont, C. Daniel, D. Baye, Three-body systems with Lagrange-mesh techniques in hyperspherical coordinates. Phys. Rev. C **67**, 044309 (2003). https://doi.org/10.1103/PhysRevC.67.044309
24. I. Brida, F. Nunes, Two-neutron overlap functions for 6he from a microscopic structure model. Nucl. Phys. A **847**, 1–23 (2010). https://doi.org/10.1016/j.nuclphysa.2010.06.012
25. C. Romero-Redondo, S. Quaglioni, P. Navrátil et al., How many-body correlations and α clustering shape ^{6}He. Phys. Rev. L **117**, 222501 (2016). https://doi.org/10.1103/PhysRevLett.117.222501
26. Z.H. Tang, J.X. Li, J.X. Ji et al., Cluster structure in Be isotopes within point-coupling covariant density functional. Chin. Phys. Lett. **30**, 012101 (2013). https://doi.org/10.1088/0256-307X/30/1/012101
27. M. Pfützner, I. Mukha, S.M. Wang, Two-proton emission and related phenomena. Prog. Part. Nucl. Phys. **132**, 104050 (2023). https://doi.org/10.1016/j.ppnp.2023.104050
28. T. Oishi, K. Hagino, H. Sagawa, Role of diproton correlation in two-proton-emission decay of the ^{6}Be nucleus. Phys. Rev. C **90**, 034303 (2014). https://doi.org/10.1103/PhysRevC.90.034303
29. T. Oishi, M. Kortelainen, A. Pastore, Dependence of two-proton radioactivity on nuclear pairing models. Phys. Rev. C **96**, 044327 (2017). https://doi.org/10.1103/PhysRevC.96.044327
30. Y.G. Ma, D.Q. Fang, X.Y. Sun et al., Different mechanism of two-proton emission from proton-rich nuclei ^{23}Al and ^{22}Mg. Phys. Lett. B **743**, 306–309 (2015)
31. M. Pfützner, I. Mukha, S.M. Wang, Two-proton emission and related phenomena. Prog. Part. Nucl. Phys. **132**, 104050 (2023). https://doi.org/10.1016/j.ppnp.2023.104050
32. S. Zhang, Y.F. Geng, F.R. Xu, Ab initio Gamow shell-model calculations for dripline nuclei. Nucl. Tech. (in Chinese) **46**, 080012 (2023). https://doi.org/10.11889/j.0253-3219.2023.hjs.46.080012
33. D.Q. Fang, H. Hua, Y.G. Ma et al., Exploring the edge of nuclear stability on the proton-rich side. Nucl. Phys. News **33**, 11–16 (2024). https://doi.org/10.1080/10619127.2023.2168911
34. Y. Kikuchi, T. Matsumoto, K. Minomo et al., Two neutron decay from the 2^+_1 state of ^{6}He. Phys. Rev. C **88**, 021602 (2013). https://doi.org/10.1103/PhysRevC.86.061602
35. L. Grigorenko, T. Wiser, K. Miernik et al., Complete correlation studies of two-proton decays: ^{6}Be and ^{45}Fe. Phys. Lett. B **677**, 30–35 (2009). https://doi.org/10.1016/j.physletb.2009.04.085
36. I. Egorova, R.J. Charity, L.V. Grigorenko et al., Democratic decay of ^{6}Be exposed by correlations. Phys. Rev. Lett. **109**, 202502 (2012). https://doi.org/10.1103/PhysRevLett.109.202502
37. L. Grigorenko, I. Egorova, R. Charity et al., Sensitivity of three-body decays to the reactions mechanism and the initial structure by example of ^{6}Be. Phys. Rev. C **86**, 061602 (2012). https://doi.org/10.1103/PhysRevC.86.061602
38. L. Grigorenko, T. Wiser, K. Mercurio et al., Three-body decay of ^{6}Be. Phys. Rev. C **80**, 034602 (2009). https://doi.org/10.1103/PhysRevC.80.034602
39. D.M. Brink, The cluster model in nuclear physics. Nucl. Phys. A **109**, 1–30 (1966). https://doi.org/10.1016/0375-9474(66)90685-5
40. A. Tohsaki, H. Horiuchi, P. Schuck et al., Alpha cluster condensation in ^{12}C. Phys. Rev. Lett. **87**, 192501 (2001). https://doi.org/10.1103/PhysRevLett.87.192501

41. K. Ikeda, M. Matsuo, H. Horiuchi, Cluster structures in light nuclei. Prog. Theor. Phys. Suppl. **123**, 773–801 (2010). https://doi.org/10.1143/PTP.123.773
42. J. Suhonen, *From Nucleons to Nucleus Concepts of Microscopic Nuclear Theory* (Springer, Berlin, 2007). https://doi.org/10.1007/978-3-540-48861-3
43. H. Horiuchi, K. Ikeda, Microscopic theory of nuclear structure. Prog. Part. Nucl. Phys. **50**, 106–142 (2003). https://doi.org/10.1016/S0146-6410(03)90039-5
44. N. Michel, J.A. Tostevin, H. Fynbo, Nuclear clustering in light nuclei. Rev. Mod. Phys. **81**, 1359–1410 (2009). https://doi.org/10.1103/RevModPhys.81.1359
45. N. Itagaki, A. Kobayakawa, S. Aoyama, New description of light nuclei by extending the amd approach. Phys. Rev. C **68**, 054302 (2003). https://doi.org/10.1103/PhysRevC.68.054302
46. Q. Zhao, B. Zhou, M. Kimura et al., Microscopic calculations of ^{6}He and ^{6}Li with real-time evolution method. Eur. Phys. J. A **58**, 25 (2022). https://doi.org/10.1140/epja/s10050-021-00648-9
47. A. Volkov, Equilibrium deformation calculations of the ground state energies of 1p shell nuclei. Nucl. Phys. **74**, 33–58 (1965). https://doi.org/10.1016/0029-5582(65)90244-0
48. R. Tamagaki, Potential models of nuclear forces at small distances. Prog. Theor. Phys. **39**, 91–107 (1968). https://doi.org/10.1143/PTP.39.91
49. N. Yamaguchi, T. Kasahara, S. Nagata et al., Effective interaction with three-body effects. Prog. Theor. Phys. **62**, 1018–1034 (1979). https://doi.org/10.1143/PTP.62.1018
50. D.Y. Tao, B. Zhou, The reduced-width amplitude in nuclear cluster physics (2024). arXiv:2412.20928 https://arxiv.org/abs/2412.20928
51. P. Descouvemont, Spectroscopic amplitudes in microscopic three-cluster systems. Phys. Rev. C **107**, 014312 (2023). https://doi.org/10.1103/PhysRevC.107.014312
52. D.Y. Tao, B. Zhou, Y.G. Ma, The 3α correlations of ground and excited 0^{+} states of ^{12}C within the microscopic cluster model (2025). arXiv:2501.10664 https://arxiv.org/abs/2501.10664
53. M. Zhukov, B. Danilin, D. Fedorov et al., Bound state properties of Borromean halo nuclei: ^{6}He and ^{11}Li. Phys. Rep. **231**, 151–199 (1993). https://doi.org/10.1016/0370-1573(93)90141-Y
54. F. Kobayashi, Y. Kanada-En'yo, Analysis of the effect of core structure upon dineutron correlation using antisymmetrized molecular dynamics. Phys. Rev. C **93**, 024310 (2016). https://doi.org/10.1103/PhysRevC.93.024310
55. C.W. Wang, B. Zhou, Y.G. Ma, Nonlocalized clustering in ^{18}O. Eur. Phys. J. A **59**, 49 (2023). https://doi.org/10.1140/epja/s10050-023-00961-5